

# On the Performance of a Novel Quasi-Synchronous Trellis-Coded CDMA System

Sangho Choe, *Member, IEEE* and Costas N. Georghiades, *Fellow, IEEE*

## Abstract

We introduce a novel signal set defined over a signal space that consists of  $L$  ( $L \geq 2$ ) orthogonal planes, and a quasi-synchronous trellis-coded code-division multiple-access (TC-CDMA) system based on it. The proposed scheme makes efficient use of the available processing gain to improve power and/or bandwidth efficiency for practical multi-user interference environments. Having a multi-planar signal constellation structure, the proposed scheme provides several options for a given required data rate, which makes it better adapted to dynamic channel conditions. Analytical bounds and simulation results indicate that at practical error rates and 2 bits/s/Hz the proposed scheme is approximately 1.2dB better than a TC-CDMA system based on 8-PSK, and 3dB better at 3 bits/s/Hz compared to TC-CDMA using 16-QAM. Additionally, the proposed system is approximately 1dB better than a multi-coded system using two signature sequences per user.

## Keywords

Trellis-coded CDMA systems, trellis-coded modulation, orthogonal plane sequence modulation (OPSM), Gaussian quadrature rule, bit error rate, pairwise error probability.

## I. INTRODUCTION

We introduce a novel trellis-coded-modulation scheme that utilizes efficiently the processing gain,  $N$ , of a code-division multiple-access (CDMA) system and a quasi-synchronous trellis-coded CDMA (QS-TC-CDMA) system based on it. There has been much work on asynchronous trellis-coded CDMA (A-TC-CDMA) systems to gain system performance by embedding trellis codes into CDMA systems, including [9], [11], and [15]. Gaudenzi and Gianneti [7] also introduce a synchronous trellis-coded CDMA (S-TC-CDMA) system for satellite communications that has a superior performance gain with respect to S-CDMA and A-TC-CDMA systems.

For perfectly synchronized and perfectly power-controlled CDMA systems, the user capacity would be the same as the processing gain  $N$  of a CDMA system [6]. However, in practical wireless channels, we cannot overlook the time-delay and power-control error due to which user capacity is substantially reduced. Ghauri and Iltis [5] show that the user capacity of S-CDMA systems is limited to  $1/9 \sim 1/6$  of the processing gain  $N$  even for a single-chip delay; Jansen and Prasad [17]

This paper was presented in part at the IEEE GLOBECOM, San Francisco, Nov. 2000.

S. Choe is with RadioCosm Inc., Mountain View, CA94043-2570 USA (e-mail: schoe@radiocosm.com).

C. N. Georghiades is with the Department of Electrical Engineering, Texas A&M University, College Station, TX77843-3128 USA (e-mail: georghia@ee.tamu.edu).

show that there is 60% user capacity loss for a 1 dB power control error and 80% for a 2.5 dB error. On the other hand, Hanly [2] and Viterbi [4] show that the user capacity,  $C$ , of synchronous CDMA systems is limited by the quality-of-service (QoS) requirement – expressed in terms of the required signal-to-interference ratio  $\alpha$  – such that  $C < N/\alpha$ . As a result, practically in conventional two-dimensional S-TC-CDMA or S-CDMA systems, one can say that we cannot fully utilize the processing gain  $N$  of a CDMA system due to the QoS requirement factor  $\alpha$ ; that is, only a small fraction of the processing gain  $N$  is utilized.

This paper introduces a multi-planar complex signaling scheme, referred to as orthogonal plane sequence modulation (OPSM)<sup>1</sup>, which for the same data rate and comparable complexity results in asymptotic coding gains with respect to conventional trellis coded modulation schemes [7] of 1.2 dB at 2 bits/s/Hz and 3.0 dB at 3 bits/s/Hz. Even comparing with multi-code S-TC-CDMA systems<sup>2</sup> based on two-dimensional signaling, which has  $L$  multiplexed code channels (orthogonal sequences) per symbol, the proposed scheme shows a superior bit-error-rate (BER) performance. Also, the multi-planar, complex, signal constellation of OPSM allows us to easily increase data rate with a negligible sacrifice in signal-to-noise ratio (SNR), thus increasing bandwidth efficiency. Another advantage of OPSM, due to the larger flexibility it offers in mapping data into the OPSM signal set, is that it can better adapt to changing data rates and other dynamic channel conditions.

OPSM is somewhat similar to the multi-dimensional trellis coded modulation (MD-TCM) of Pietrobon et al. [13], having  $L \times MPSK$ , in the sense that they both are multi-dimensional. However, while OPSM has a single signal point for each time instant, MD-TCM has multiple ( $L$ ). So, the effective spreading gain per signal point of MD-TCM reduces to  $N/L$ . This is partly why in the context of CDMA MD-TCM has been shown not to provide a performance improvement with respect to conventional CDMA systems [12].

In Section II, we introduce the orthogonal plane sequence modulation schemes (OPSM) and its features. In Section III, the system model and performance analysis of the quasi-synchronous trellis-coded CDMA (QS-TC-CDMA) system based on OPSM is dealt with. Section IV includes performance analysis results and Section V numerical results for our QS-TC-CDMA system; finally, we conclude with Section VI.

<sup>1</sup>In this paper we will keep this term even for pseudo-orthogonal sequences like Gold sequences.

<sup>2</sup>IS-95 standard upgrades to IS-95B standard by adopting multi-code CDMA (MC-CDMA) [21].

## II. ORTHOGONAL PLANE SEQUENCE MODULATION

The OPSM signal space consists of  $L$  orthogonal signal planes, each containing uniformly distributed signal points. Each signal plane is identified by its own unique signature sequence, called the plane signature sequence (PSS). One OPSM signal point can be represented by the PSS of the signal plane on which that signal point lies along with the phase and amplitude of that signal point.

In this paper we confine the amplitude of OPSM signal points in each plane to be constant, thus focusing on phase-shift keying (PSK) signaling. We will denote OPSM signaling using  $L$  planes with  $M$ -PSK constellations on each plane as  $LPMP$ SK. The  $m$ -th phased signal point on the  $l$ -th OPSM signal plane, denoted by a complex vector  $\mathbf{u}_{l,m}$ , is represented as:

$$\mathbf{u}_{l,m} = \mathbf{a}_l e^{j\phi_m}, \quad l = 0, \dots, L-1, \quad m = 0, \dots, M-1,$$

where  $\mathbf{a}_l = \{a_{l,0}, a_{l,1}, \dots, a_{l,N-1}\}$  is the PSS of the  $l$ -th signal plane and  $\phi_m$  is the phase of the  $m$ -th PSK signal on that signal plane. Fig. 1 shows the 2P4PSK signal constellation that consists of two signal planes, each containing a 4-PSK constellation. Clearly, each modulation symbol in OPSM is in fact a complex signature sequence, combining spreading and modulation. The overall alphabet size,  $A$ , of the  $LPMP$ SK OPSM signal constellation is  $A = L \cdot M$ . Note that for a certain data rate, with an alphabet size  $A$  there are several combinations (options) of  $L$  and  $M$  available. For example, for  $A = 8$ , there are 1P8PSK ( $L = 1, M = 8$ ), 2P4PSK ( $L = 2, M = 4$ ), and 4P2PSK ( $L = 4, M = 2$ ). The availability of choice makes OPSM more adaptable to channel conditions.

Theorem 1 in Appendix A states and proves that the signal constellation,  $S$ , corresponding to OPSM is geometrically uniform. This guarantees a uniform decision region (Voronoi region [14]) for any signal point  $s \in S$ , resulting in the same Euclidean distance profiles for all signal points in  $S$ . While conventional two-dimensional modulation schemes, including  $M$ -PSK and  $M$ -QAM, form a two-dimensional real lattice  $Z^2$ , the OPSM signal set becomes a  $2L$ -dimensional real lattice  $Z^{2L}$  because its signal space is  $L$ -planar. Thus, the set partitioning of OPSM concerns the *geometrically uniform* partitioning over the real  $2L$ -dimensional Euclidean signal space  $\mathbb{R}^{2L}$ . Letting the original signal set of OPSM be a lattice  $S$ , the sub lattice  $S'$  and its cosets are obtained by the set partitioning  $S/S'$ .

Corollary 1 in Appendix A states that the OPSM signal set has the *isometric labelling* property by which the binary input vector one-to-one maps into the signal set. Based on the *isometric labeling*, we can one-to-one map a binary vector into the generalized OPSM signal  $LPMP$ SK. For the order  $n$  binary labeling vector – also called the signal mapper input vector, the  $k$  bits differentiate  $M = 2^k$  signal phases of the modulation symbol and the remaining  $l$  bits,  $l = n - k$ , of that vector, also

called the PSS bits, differentiate the  $L = 2^l$  signal planes of that symbol. But we need to assign the  $l$  PSS bits in a judicious manner such that the signal set could be maximally separated through set partitioning. Assuming an  $(n, k)$  convolutional code, the partitioning proceeds at each level in an increasing order from level 0 to  $n - 1$ , such that maximally separated subsets are obtained on each level [1].

In set-partitioning the OPSM set, two different signal planes are separated by one PSS bit. While for 2P4PSK the plane separation can occur at any level, even at level 0, because of the same distance profiles for each constellation point, for 2P8PSK the plane separation should occur at a level higher than level 0, in order to maximally separate the signal set. For instance, Fig. 1 shows the binary labeling for 2P4PSK and Fig. 2 shows its set partitioning scheme. The first 2 bits differentiate 4-phased signals and the last bit (the PSS bit) differentiates the two signal planes: e.g. a labeling vector 6 ('110') indicates the 4th phased signal of the 1st signal plane and a labeling vector 3 ('011') indicates the 3rd phased signal of the 2nd signal plane.

### III. SYSTEM MODEL

As shown in Fig. 3, the transmitter is composed of a convolutional encoder and a signal mapper. The signal mapper has both the set partitioning function which, based on the input vector, selects a signal subset from the entire signal set and the signal selection function which selects a signal from the signal subset. In other words, the signal mapper receives an output vector from the convolutional encoder, which consists of  $k_2$  uncoded bits and  $n$  coded bits, then maps this vector into a modulation symbol from the OPSM signal set. In order to generate the pseudo-orthogonal plane signature sequence (PSS), we have a *preferentially-phased Gold-sequence* generator [8].

Assuming the  $l$ th plane,  $m$ th phase symbol vector of the  $k$ th user,  $\mathbf{u}_{l,m}^k$ , is transmitted, its corresponding signal on the time-axis, denoted by  $u_{l,m}^k(t)$ , can be represented as

$$u_{l,m}^k(t) = A_l^k(t)e^{j\phi_m^k} = e^{j\phi_m^k} \sum_{n=0}^{N-1} a_{l,n}^k p_{T_c}(t - nT_c) \quad (1)$$

where  $l = 0, \dots, L - 1$  and  $m = 0, \dots, M - 1$ .  $A_l^k(\cdot)$  represents the time-axis PSS of a modulation signal,  $\phi_m^k$  represents the signal phase,  $T_c$  is the chip period, and  $p_{T_c}(\cdot)$  is the chip waveform function. Then, the corresponding transmit signal of the  $k$ th user is given by

$$\begin{aligned} s_{l,m}^k(t) &= \sqrt{2P} \Re \left\{ u_{l,m}^k(t) e^{j(w_c t + \theta^k)} \right\} \\ &= \sqrt{2P} \Re \left\{ e^{j(w_c t + \phi_m^k + \theta^k)} \sum_{n=0}^{N-1} a_{l,n}^k p_{T_c}(t - nT_c) \right\} \end{aligned} \quad (2)$$

where  $P$  is the signal power and  $\theta^k$  is the phase delay of the  $k$ th user signal.

For the time being and for simplicity we will suppress the signal indices  $m$  and  $l$ . Assuming an AWGN channel with two-sided spectral density  $N_0/2$ , the received signal, which is the sum of all  $K$  user signals, can be represented by

$$r(t) = \sum_{k=1}^K s^k(t - \tau^k) + n(t) \quad (3)$$

in which the time delay of the  $k$ th user is  $\tau^k$ .

We assume a conventional, coherent, matched-filter receiver. At the receiver, the received signal  $r(t)$  is cross-correlated with a bank of  $2L$  correlators as shown in Fig. 4. The soft decision output vector obtained from the bank of correlators is decoded by a Viterbi decoder. Let us assume that User  $i$ 's signal is the desired signal to be recovered. Let the matched-filter bank vector for User  $i$  be:

$$\mathbf{Y}^i = \{Y_j^i; j = 0, \dots, L-1\}.$$

Each complex element of the matched-filter output vector at the  $i$ th user receiver can be represented by

$$\begin{aligned} Y_0^i &= \sqrt{\frac{2}{T_s}} \int_0^{T_s} r(t) e^{-jw_c t} \left[ \sum_{n=0}^{N-1} a_{0,n}^i p_{T_c}(t - nT_c) \right] dt \\ &\vdots \\ Y_{L-1}^i &= \sqrt{\frac{2}{T_s}} \int_0^{T_s} r(t) e^{-jw_c t} \left[ \sum_{n=0}^{N-1} a_{L-1,n}^i p_{T_c}(t - nT_c) \right] dt. \end{aligned}$$

Without loss of generality, we assume that the time delay  $\tau^i$  of User  $i$  is zero and a signal on the  $l$ th plane,  $l = 0, \dots, L-1$ , of the  $k$ th user is transmitted. The correlator output vector for User  $i$  at the  $p$ th instance is

$$\begin{aligned} \mathbf{Y}_p^i &= \{Y_{j,p}^i; j = 0, \dots, L-1\} \\ &= \frac{\sqrt{E_s}}{T_s} e^{j\phi_p^i} \mathbf{R}^{i,i}(0) + \frac{\sqrt{E_s}}{T_s} \sum_{k=1, k \neq i}^K \left\{ \mathbf{R}^{i,k}(\tau^k) e^{j\beta_{p-1}^k} \right. \\ &\quad \left. + \tilde{\mathbf{R}}^{i,k}(\tau^k) e^{j\beta_p^k} \right\} + \boldsymbol{\eta}_p^i \end{aligned} \quad (4)$$

in which the signal phase of the  $k$ th user is  $\beta_p^k = \phi_p^k + \theta^k - w_c \tau^k = \phi_p^k + \theta^{k'}$ ;  $\mathbf{R}^{i,i}(\cdot)$  is the autocorrelation vectors of size  $L$  and  $\mathbf{R}^{i,k}(\cdot)$  and  $\tilde{\mathbf{R}}^{i,k}(\cdot)$  are the even and odd continuous-time

partial cross-correlation vector of size  $L$ , respectively, due to the time delay  $\tau^k$  [16], [9]. Assuming a transmit signal on the  $l$ th plane of User  $i$ , the autocorrelation function of (4) can be described by

$$\mathbf{R}^{i,i}(0) = \{R_{j,l}^{i,i}(0); j = 0, \dots, L-1\} \quad (5)$$

where

$$R_{j,l}^{i,i}(0) = \begin{cases} NT_c(=T_s), & \text{for } j = l \text{ (same plane)} \\ -T_c, & \text{for } j \neq l \text{ (different plane)} \end{cases}$$

Also, in (4), the odd continuous-time partial cross-correlation vector can be defined [16] by

$$\tilde{\mathbf{R}}^{i,k}(\tau^k) = \left\{ \tilde{R}_{j,l}^{i,k}(\tau^k); j = 0, \dots, L-1 \right\} \quad (6)$$

where

$$\begin{aligned} \tilde{R}_{j,l}^{i,k}(\tau^k) &= \int_{\tau^k}^{T_s} a_j^i(t) a_l^k(t - \tau^k) dt \\ &= C_{j,l}^{i,k}(m) \tilde{R}_\psi(\tau^k - mT_c) \\ &\quad + C_{j,l}^{i,k}(m+1) R_\psi(\tau^k - mT_c) \end{aligned}$$

in which  $a_x^y(\cdot)$  indicates the  $y$ th user  $x$ th PSS.  $C_{j,l}^{i,k}(u)$  is an aperiodic cross-correlation function for the  $u$ th ( $u$  is a positive integer) chip delay between the  $i$ th user  $j$ th PSS and the  $k$ th user  $l$ th PSS, and  $R_\psi(\cdot)$  and  $\tilde{R}_\psi(\cdot)$  are the partial autocorrelation functions of the chip waveform signal, following the definitions in [16], [9]. Likewise, the even continuous-time partial cross-correlation vector function [16] can be defined but is omitted here.

For simplicity, we assume that the cross-correlation characteristics between two different users with different PSS's are the same as those between two different users using the same PSS. This can be justified from the fact that the cross-correlation between two different user signature sequences does not depend much on the plane index, because of the pseudo-orthogonality between two different user signature sequences. Hence we can drop the plane indices from  $\mathbf{R}^{i,k}(\cdot)$  and  $\tilde{\mathbf{R}}^{i,k}(\cdot)$ .

In our QS-TC-CDMA system, let us assume that the time delay  $\tau$  has been limited to within a chip period such that  $|\tau| \leq 0.5T_c$ . Also assume that the partial cross-correlation function between two sequences is symmetrical with respect to  $\tau = 0$  and  $\tau$  is uniformly-distributed for that chip period. Then, without loss of generality we can just take the positive period of  $\tau$  such that (4) can be further simplified just with the odd continuous-time partial cross-correlation function  $\tilde{\mathbf{R}}^{i,k}(\cdot)$

(see (6)) as follows:

$$\begin{aligned} \mathbf{Y}_p^i &\simeq \frac{\sqrt{E_s}}{T_s} e^{j\phi_p^i} \mathbf{R}^{i,i}(0) + \frac{\sqrt{E_s}}{T_s} \mathbf{1} \\ &\quad \cdot \sum_{k=1, k \neq i}^K \{ \tilde{R}^{i,k}(\tau^k) e^{j\phi_p^k} e^{j\theta^k} \} + \boldsymbol{\eta}_p^i \end{aligned} \quad (7)$$

$$= \mathbf{G}_p^i + \mathbf{V}_p^i + \boldsymbol{\eta}_p^i \quad (8)$$

in which  $\mathbf{G}_p^i$  is the desired signal (User  $i$ ) symbol vector,  $\mathbf{V}_p^i$  is the other user interference vector that has a column vector  $\mathbf{1} = (1, 1, \dots, 1)^T$  of size  $L$ , and  $\boldsymbol{\eta}_p^i$  is the noise vector whose elements on each plane have variance  $N_0/2$ .

#### IV. PERFORMANCE ANALYSIS

##### A. Perfectly-Synchronous CDMA System based on OPSM

In the perfectly-synchronous CDMA system, there assumes no time delay:  $\tau^k = 0$  for any  $k$ . Let us assume that a signal on the  $l$ th plane of User  $i$  will be recovered. Under the condition of perfect synchronism, the cross-correlation value,  $R^{i,k}(0)$ , of the *preferentially-phased Gold sequence* is equal to  $-T_c$  for  $k \neq i$  [8]. Thus, User  $i$ 's channel output symbol vector of (7) at the  $p$ th instance can be rewritten as

$$\mathbf{Y}_p^i = \{Y_{j,p}^i; j = 0, \dots, L-1\} \quad (9)$$

where

$$\begin{aligned} Y_{j,p}^i &\simeq \begin{cases} \sqrt{E_s} e^{j\phi_p^i} - \frac{T_c \sqrt{E_s}}{T_s} \sum_{\substack{k=1 \\ k \neq i}}^K e^{j\beta_p^k} + \eta_{j,p}^i & \text{for } j = l \\ -\frac{T_c \sqrt{E_s}}{T_s} e^{j\phi_p^i} - \frac{T_c \sqrt{E_s}}{T_s} \sum_{\substack{k=1 \\ k \neq i}}^K e^{j\beta_p^k} + \eta_{j,p}^i & \text{for } j \neq l \end{cases} \\ &= G_{j,p}^i + V_{j,p}^i + \eta_{j,p}^i \end{aligned}$$

in which  $j = 0, \dots, L-1$  and  $\beta_p^k = \phi_p^k + \theta^k$ ; the phase delay  $\theta^k$  of the  $k$ th user is assumed to be uniformly distributed in  $[0, 2\pi]$ .

Based on the channel output vector in (9), we can obtain the Chernoff bound on the pairwise error probability, described in detail in Appendix B, in a simple closed-form expression as follows:

$$\begin{aligned} p(\mathbf{g} \rightarrow \tilde{\mathbf{g}}) &\leq \prod_{p \in \mathcal{C}} \exp \left[ -\lambda(1-\lambda) \frac{E_s}{N_0} \|\mathbf{g}_p - \tilde{\mathbf{g}}_p\|^2 \right] \\ &\quad \cdot \exp \left\{ \left( \frac{\lambda}{N} \right)^2 \left( \frac{E_s}{N_0} \right)^2 (K-1) \|\mathbf{g}_p - \tilde{\mathbf{g}}_p\|^2 \right\}. \end{aligned} \quad (10)$$

To tighten the bound, the optimum value of the Chernoff parameter  $\lambda$ ,  $\lambda_{opt}$ , is:

$$\lambda_{opt} = \frac{1}{2\{1 + \frac{(K-1)E_s}{N^2} \frac{E_s}{N_0}\}}. \quad (11)$$

For a moderate range of signal-to-noise ratios (6 dB  $\sim$  12 dB) and  $N \gg K$ ,  $\lambda_{opt}$  is approximately the same as the Bhattacharyya value of 1/2.

### B. Quasi-Synchronous CDMA System based on OPSM

The time delay  $\tau^k$  in the quasi-synchronous system has been limited to within a chip period such that  $|\tau^k| \leq 0.5T_c$  for  $k = 1, \dots, K$  and  $k \neq i$ . Thus the desired user (User  $i$ ) channel output symbol vector of (7) at the  $p$ th instance can be rewritten as

$$\mathbf{Y}_p^i = \{Y_{j,p}^i; j = 0, \dots, L-1\} \quad (12)$$

where

$$Y_{j,p}^i \simeq \begin{cases} \sqrt{E_s} e^{j\phi_p^i} + \frac{\sqrt{E_s}}{T_s} \sum_{\substack{k=1 \\ k \neq i}}^K \tilde{R}^{i,k}(\tau^k) e^{j\beta_p^k} + \eta_{j,p}^i & \text{for } j = l \\ -\frac{T_c \sqrt{E_s}}{T_s} e^{j\phi_p^i} + \frac{\sqrt{E_s}}{T_s} \sum_{\substack{k=1 \\ k \neq i}}^K \tilde{R}^{i,k}(\tau^k) e^{j\beta_p^k} + \eta_{j,p}^i & \text{for } j \neq l \end{cases}$$

$$= G_{j,p}^i + V_{j,p}^i + \eta_{j,p}^i.$$

The time delay has a range of  $-T_c/2 \leq \tau^k \leq T_c/2$  and the phase term becomes  $\beta_p^k = \phi_p^k + \theta^k$ , and the phase delay  $\theta^k$  of the  $k$ th user is assumed to be uniformly distributed in  $[0, 2\pi]$ . Let us assume that we use a rectangular chip waveform signal. Then the odd continuous-time partial cross-correlation term of (6) [16], with dropping plane indices, becomes

$$\tilde{R}^{i,k}(\tau^k) = \{(T_c - \tau^k)C^{i,k}(0) + \tau^k C^{i,k}(1)\}$$

where  $C^{i,k}(0) = -1$ .

In the quasi-synchronous system, it is not easy to obtain a simple closed-form expression for the pairwise error probability since the cross-correlation function also depends on the user index  $k$ . Thus, we utilize the method of moments – also called the Gaussian quadrature rule (GQR) [18] – to obtain a performance bound. The pairwise error probability for quasi-synchronous systems,

derived in Appendix B, is then:

$$p(\mathbf{g} \rightarrow \tilde{\mathbf{g}}) \leq \prod_{p \in C} \exp \left[ -\lambda(1-\lambda) \frac{E_s}{N_0} \|\mathbf{g}_p - \tilde{\mathbf{g}}_p\|^2 \right] \cdot \sum_{j=1}^{N_c} W_{j,p} \exp \left( -2\lambda \frac{E_s}{N_0} \zeta_{j,p} \right). \quad (13)$$

We need to optimize  $\lambda$  in order to tighten the bound. However, it should be noted that  $\lambda$  is also dependent on the sequence length  $N$ ; thus we can use a numerical approach to compute the optimum Chernoff parameter,  $\lambda_{opt}$ . Asymptotically, one can assume that  $\lambda$  can be optimized over the branch with minimum distance, and this value can be applied to all branches. Even so, the degradation in tightness of the Chernoff bound is not significant [10].

### C. Gaussian Approximation

In CDMA environments, as the number of users in a cell increases, the multiuser interference becomes Gaussian. Under this assumption, the second expectation on the right hand side of (19) Appendix B can be approximated as follows:

$$E \left\{ \exp \left[ -2\lambda E_s \sum_{l=0}^{L-1} \Re \{ v_{l,p} (g_{l,p} - \tilde{g}_{l,p})^* \} \right] \right\} \approx \exp (2\lambda^2 E_s^2 \sigma_v^2 \|\mathbf{g}_p - \tilde{\mathbf{g}}_p\|^2) \quad (14)$$

in which the variance of interference at each plane is  $\sigma_v^2 = \sigma_{v_l}^2 = 1/2E\{|v_{l,p}|^2\}$ ,  $l = 0, \dots, L-1$ . By substituting (14) into (19) and replacing the Chernoff parameter  $\lambda$  with its optimum value

$$\lambda_{opt} = \frac{1}{4(N_0/2 + \sigma_v^2 E_s)} \quad (15)$$

one can obtain the pairwise error probability given by

$$p(\mathbf{g} \rightarrow \tilde{\mathbf{g}}) \leq \prod_{p \in C} \exp \left\{ -\frac{\|\mathbf{g}_p - \tilde{\mathbf{g}}_p\|^2}{4(N_0/E_s + E[|v_p|^2])} \right\} \quad (16)$$

where

$$E[|v_p|^2] = \begin{cases} \frac{(K-1)}{N^2}, & \text{for } |\tau^k| = 0 \\ \frac{(K-1)}{N^2} E[\{\tilde{R}^{i,k}(\tau^k)\}^2], & \text{for } |\tau^k| < T_c \end{cases}$$

Note that equation (16) is the same as  $M$ -PSK [9] except for the  $2L$ -dimensional distance metrics.

## V. NUMERICAL RESULTS

In this section, the performance of the QS-TC-CDMA system based on OPSM is numerically analyzed. The results show that OPSM is an efficient modulation scheme that improves BER

performance and/or increases throughput efficiency in CDMA systems with a limited user capacity  $C < N/\alpha$ , where  $\alpha$  is the QoS requirement factor [2], [4].

To compute BER results, we need to obtain the generalized transfer function  $T(Z, I)$  based on the product trellis of the trellis-coded system and then use [19], [20]

$$P_b \leq \frac{1}{n} \frac{\partial \bar{T}(Z, I)}{\partial Z} \Big|_{Z=1}$$

where  $n$  is the number of bits per symbol and the overbar indicates that the transfer function bound has been averaged over the interuser interference.

We employ Ungerboeck's systematic convolutional encoders with feedback [1]. Specifically, we use 4-state rate 1/2 and 8-state rate 2/3 convolutional codes in our analysis. As a pseudo-random sequences, we use the *preferentially-phased Gold-sequences* [7] whose sequence length is assumed  $N = 31$  or  $N = 63$ .

Fig. 5 and Fig. 6 show the BER performance of a quasi-synchronous 2/3 2P4PSK TC and a quasi-synchronous 3/4 2P8PSK TC, respectively, as a function of the number of users  $K$ ; the convolutional code implemented into both systems is an 8-state rate 2/3 code and the sequence length is  $N = 63$ . For a BER of  $10^{-7}$  the required SNR for the 2P4PSK TC for  $K = 7$  is 9.2 dB and that of the 2P8PSK TC is 8.3 dB.

In Fig. 7 we compare the theoretical Chernoff bounds with simulation results for the rate 2/3 2P4PSK TC. For  $K = 7$  users and  $N = 63$ , Fig. 7 shows the performance of quasi-synchronous 2P4PSK TC for both the four and eight state codes. We see that the upper bound for the 8-state code is somewhat tighter than for the 4-state code, but the difference is small. Fig. 7 also shows Gaussian approximation (GA) results for the 4-state and 8-state codes. These results match closely the Chernoff bound at low SNRs, but not as well at high SNRs.

The BER performance of OPSM is compared to conventional schemes, including  $M$ -PSK TC and  $M$ -QAM TC [7]. For a fair comparison we assume that both systems have the same complexity and same processing gain. Fig. 8 compares the perfectly-synchronous rate 2/3 2P4PSK TC and perfectly-synchronous rate 2/3 8-PSK TC for  $R_b = 2$  bits/s/Hz and compares the perfectly-synchronous rate 3/4 4P4PSK TC, perfectly-synchronous rate 3/4 2P8PSK, and perfectly-synchronous rate 3/4 16-QAM TC [7] for  $R_b = 3$  bits/s/Hz; we assume that all schemes for  $R_b = 2$  bits/s/Hz and  $R_b = 3$  bits/s/Hz employ the same 8-state rate 2/3 convolutional code. For a processing gain  $N = 31$  and  $K = 14$  users, we observe that 2P4PSK TC has a 1.2 dB gain compared to 8-PSK TC at a  $10^{-5}$  BER. For the same conditions, the gain of 4P4PSK TC and 2P8PSK TC compared to 16-QAM TC is 4.0 dB and 3.7 dB, respectively, for a  $10^{-5}$  BER; that is, as data rate increases, the

performance gain of OPSM schemes over existing schemes increases. As another point, whereas in order to increase data rate from 2 bits/s/Hz to 3 bits/s/Hz existing schemes sacrifice 2.9 dB SNR based on  $10^{-5}$  BER, for OPSM schemes there is no SNR sacrifice (4P4PSK TC) or 0.4 dB SNR sacrifice (2P8PSK TC). As a result, OPSM does not only provide a superior bandwidth efficiency compared to conventional schemes, but also provides several options (3 for 3 bits/s/Hz including 1P16QAM) for a single data rate without changing any system structure. Then, we can choose a proper option depending on the channel conditions and QoS requirements.

In Fig. 8, we also show results of a multi-code TC-CDMA system based on conventional signaling (8-PSK) that occupies two-multiplexed code channels per user signal, increasing its processing gain by a factor of two ( $2N$ ). Multi-code systems, however, also make the intercode interference increased by the same factor (two for this example). Thus, our OPSM based system (2P4PSK TC) still achieves superior performance over the multi-code 8-PSK TC system, e.g. 0.9 dB gain based on a  $10^{-5}$  BER.

For a fair spectral efficiency comparison between CDMA systems we compare BER performance in terms of the system loading for which the normalized offered traffic  $L = R_b * K/N$  [15], where  $K$  is the number of users, is defined. Fig. 9 shows BER performance versus  $L$  between quasi-synchronous conventional TC-CDMA systems, quasi-synchronous multi-code TC-CDMA systems, and quasi-synchronous OPSM TC-CDMA systems, where we assume  $E_b/N_0 = 8$  dB,  $N = 31$ , and the same 8 state 2/3 convolutional codes. One can observe that OPSM based TC system outperforms the conventional TC or multi-code TC systems. Note that under the same system loading the system performance 4P4PSK TC is superior to 2P4PSK TC as well as 2P8PSK TC.

## VI. CONCLUSION

We introduced a modulation scheme, orthogonal plane sequence modulation (OPSM), and a QS-TC-CDMA system based on it. OPSM has been shown to be an efficient modulation scheme that results in improved power and/or bandwidth efficiency in CDMA systems which operate at user capacities lower than the processing gain.

For the same processing gain and decoding complexity, the asymptotic coding gain of OPSM with respect to conventional S-TC-CDMA schemes is 1.2 dB at 2 bits/s/Hz and 3.0 dB at 3 bits/s/Hz, respectively. Compared to a multi-code S-TC-CDMA system based on two-dimensional signaling that has  $L$  multiplexed code channels per symbol, the BER performance of the proposed scheme is superior.

With OPSM, data rate increase incurs a relatively small sacrifice in signal-to-noise ratio compared

to existing schemes. Furthermore, depending on dynamic channel conditions, OPSM allows us to choose the best scheme, in a distance sense, among several options for a certain data rate, without changing the system structure. Hence, the proposed scheme would be more robust.

## APPENDIX A

### GEOMETRIC UNIFORMITY AND ISOMETRIC LABELING

Let us assume that the signal set on one signal plane of OPSM,  $M$ -PSK, is *geometrically uniform* over the signal sample space  $\mathbb{R}^2$  [14] and is congruent with each of the other signal planes. Thus, we only need to verify that the OPSM signal set, having  $L$  ( $L \geq 2$ ) signal planes, still preserves *geometrical uniformity*.

*Theorem 1 (Geometrical uniformity)* The OPSM signal set  $S$  is *geometrically uniform*, that consists of  $L$  ( $= 2^l$ ,  $l$  is positive integer) signal planes:  $S = S_0 + S_1 + \dots + S_{L-1}$ , in which  $S_i$  ( $i = 0, \dots, L-1$ ) is the  $i$ th signal plane.

*Proof:* The OPSM signal set  $S$  is *geometrically uniform* if there is a transitive symmetry group  $\Gamma(S)$  [14]. Denote the signal set in plane 0 as  $S_0$ ; under the assumption, this *geometrically uniform* set has a transitive symmetry group  $\Gamma_1 = R_M$ , which is a set of rotations by multiples of  $360^\circ/M$ .  $S_0$  and  $S_1$  have a reflection isometry (two-element reflection group)  $V$  since they are congruent; so the combined set  $Y_1 = S_0 \cup S_1$  forms a transitive symmetry group  $\Gamma_2 = V \cdot R_M$ . Also the set  $Y_1$  has a reflection isometry  $V$  with a set  $Y_2 = S_2 \cup S_3$  so that the combined set  $Y_1 \cup Y_2$  forms a new transitive symmetry group  $\Gamma_3 = V^2 \cdot R_M$ . Repeating these same procedures, finally we can obtain the transitive symmetry group  $\Gamma(S) = \Gamma_{l+1} = V^l \cdot R_M$ , where  $l = \log_2(L)$  for  $L \geq 2$ . ■

*Definition 1:* *Geometrically uniform* signal set  $S$  that has a transitive symmetry group  $\Gamma(S)$  has the one-to-one label map (*isometric labeling*)  $m: A \rightarrow S/S'$ , where  $A$  is the binary input label group,  $S/S'$  is a partition of  $S$ , and  $S'$  is the subset obtained by ‘mapping by set partitioning’ [14].

*Corollary 1:* The OPSM signal set has the one-to-one label map (*isometric labeling*).

Let us denote the generalized OPSM signal as  $LPMP$ SK. Then the symmetry group  $\Gamma(S)$  to generate OPSM is  $R_M \cdot V^l$  (see *Theorem 1*), where  $l = \log_2 L$  and  $M = 2^k$  and  $k$  is a positive integer. The group  $R_M$  is isomorphic to  $Z_M = (Z_2)^k$  (binary labeling) and the group  $V$  is isomorphic to  $Z_2$ . Thus one can map the elements of the binary label group  $A = Z_M \cdot (Z_2)^l$ , that is isomorphic to  $\Gamma(S)$ , into the signals of signal set  $S$  and its mapping is one-to-one (*isometric labeling*).

## APPENDIX B

## PAIRWISE ERROR PROBABILITY

Let us derive the Chernoff bound [20], [9], [19], of the pairwise error probability of the OPSM QS-TC-CDMA system, based on the channel output signal vector (7). Let us assume a  $L$ -planar OPSM signal is transmitted. Let us define the transmit (or channel input) symbol sequence of length  $N_s$ ,  $\mathbf{G} = \{\mathbf{G}_1, \mathbf{G}_2, \dots, \mathbf{G}_{N_s}\}$ , in which  $\mathbf{G}_p$  is the transmit symbol at the  $p$ th time instance. Assuming the other user interference vector  $\mathbf{V}$  is known, the optimum metric under a AWGN channel becomes

$$P(\mathbf{G} \rightarrow \tilde{\mathbf{G}}|\mathbf{V}) \leq \prod_{p \in C} E \left[ \exp\{\lambda(\|\mathbf{Y}_p - \mathbf{G}_p\|^2 - \|\mathbf{Y}_p - \tilde{\mathbf{G}}_p\|^2)\} \right] \quad (17)$$

in which  $\mathbf{Y}_p = \{Y_{0,p}, Y_{1,p}, \dots, Y_{L-1,p}\}$  and  $\mathbf{G}_p = \{G_{0,p}, G_{1,p}, \dots, G_{L-1,p}\}$  are the channel output symbol vector and the channel input symbol vector, respectively, and  $C$  is the set of path  $p$  such that  $\mathbf{G} \neq \tilde{\mathbf{G}}$ . And its distance measure at the  $p$ th instance is

$$\|\mathbf{Y}_p - \mathbf{G}_p\|^2 = \sum_{l=0}^{L-1} |Y_{l,p} - G_{l,p}|^2. \quad (18)$$

Let us substitute (18) into (17) and normalize  $\mathbf{G}_p$  and  $\mathbf{V}_p$  (the interference symbol vector) by the symbol magnitude  $\sqrt{E_s}$  such that  $\mathbf{g}_p = \mathbf{G}_p/\sqrt{E_s}$  and  $\mathbf{v}_p = \mathbf{V}_p/\sqrt{E_s}$ ; and reorganizing (17) gives [9]

$$\begin{aligned} P(\mathbf{g} \rightarrow \tilde{\mathbf{g}}|\mathbf{v}) &\leq \prod_{p \in C} \exp(\lambda E_s \sum_{l=0}^{L-1} (|g_{l,p} - \tilde{g}_{l,p}|^2)) \\ &\quad \cdot E\{\exp[-2\lambda\sqrt{E_s} \sum_{l=0}^{L-1} \Re\{\eta_l(g_{l,p} - \tilde{g}_{l,p})^*\}]\} \\ &\quad \cdot E\{\exp[-2\lambda E_s \sum_{l=0}^{L-1} \Re\{v_{l,p}(g_{l,p} - \tilde{g}_{l,p})^*\}]\}. \end{aligned} \quad (19)$$

The first expectation on the right hand of (19) that has a complex Gaussian random variable  $\eta_l = \eta_l^I + j\eta_l^Q$ , whose variances are  $\text{var}\{\eta_l\} = \text{var}\{\eta_l^I\} = \text{var}\{\eta_l^Q\} = N_0/2$ , becomes [9]

$$\begin{aligned} &E\{\exp[-2\lambda\sqrt{E_s} \sum_{l=0}^{L-1} \Re\{\eta_l\{g_{l,p} - \tilde{g}_{l,p}\}^*\}]\} \\ &= \exp\{N_0 E_s \lambda^2 \|\mathbf{g}_p - \tilde{\mathbf{g}}_p\|^2\}. \end{aligned}$$

The remaining derivations for a perfectly-synchronous and a quasi-synchronous CDMA system, including the second expectation on the right hand side of (19), follow, respectively, in the next two subsections.

### B.1 Perfectly-Synchronous CDMA System

First, let us normalize the interference term in (9),  $v_{j,p}^i = V_{j,p}^i/\sqrt{E_s}$ , and drop the plane index  $j$ , without loss of generality, as mentioned before in Section III; and substitute it into the second expectation on the right hand side of (19). Let us assume that the source information is equally-probable and is symbol-by-symbol independent. Hence, the second expectation on the right hand side of (19) is given by

$$\begin{aligned} & E \left\{ \exp \left[ -2\lambda E_s \sum_{l=0}^{L-1} \Re\{v_{l,p}(g_{l,p} - \tilde{g}_{l,p})^*\} \right] \right\} \\ &= \left[ E \left\{ \exp \left[ \alpha \Re\{e^{j\beta_p} \boldsymbol{\delta}_p^*\} \right] \right\} \right]^{K-1} = I_0(\alpha \|\boldsymbol{\delta}_p\|)^{K-1} \end{aligned} \quad (20)$$

where  $\alpha = 2\lambda E_s/N$  and  $\boldsymbol{\delta}_p = \boldsymbol{\delta}_{rp} + j\boldsymbol{\delta}_{ip} = \mathbf{g}_p - \tilde{\mathbf{g}}_p$ ;  $\mathbf{g}_p$  and  $\tilde{\mathbf{g}}_p$  are the normalized versions of  $\mathbf{G}_p$  and  $\tilde{\mathbf{G}}_p$  by  $\sqrt{E_s}$ , respectively,  $\lambda$  is the Chernoff parameter, and  $I_0(\cdot)$  is the *zeroth order modified Bessel function*.

Hence, from (19), by letting  $\lambda' = \lambda/N_0$  and dropping the primes, the pairwise error probability bound of the perfectly-synchronous CDMA system can be obtained as follows:

$$\begin{aligned} p(\mathbf{g} \rightarrow \tilde{\mathbf{g}}) &\leq \prod_{p \in C} \exp \left[ -\lambda(1-\lambda) \frac{E_s}{N_0} \|\mathbf{g}_p - \tilde{\mathbf{g}}_p\|^2 \right] \\ &\quad \cdot \prod_{l=0}^{L-1} [I_0(\beta_l)]^{K-1} \end{aligned} \quad (21)$$

where

$$\beta_l = \frac{2\lambda E_s}{N N_0} |g_{l,p} - \tilde{g}_{l,p}|.$$

Under the assumption of  $E_s/N_0 \ll N$  ( $\beta_l \leq 1$ ) we can approximate (21) well by utilizing  $\ln(I_0(\beta_l)) \simeq 1/4\beta_l^2$ . Thus, rewriting (21) results in a simple closed-form expression (10).

### B.2 Quasi-Synchronous CDMA System

First, let us normalize the interference term in (12),  $v_{j,p}^i = V_{j,p}^i/\sqrt{E_s}$ , and drop the plane index  $j$ , without loss of generality, as mentioned before in Section III. Substituting the normalized

interference term into the second expectation on the right hand side of (19) yields

$$\begin{aligned}
& E\{\exp[-2\lambda E_s \Re\{v_p^i \boldsymbol{\delta}_p^*\}]\} \\
&= E\left\{\exp\left[-\alpha \sum_{k=1, k \neq i}^K \left\{ (C^{i,k}(1)+1) \tau^k - 1 \right\} \Re\left\{ \boldsymbol{\delta}_p^* e^{j(\phi_p^k + \theta^k)} \right\} \right]\right\} \\
&= E\{\exp(-\alpha \mathbf{y}_p)\}
\end{aligned} \tag{22}$$

where

$$\mathbf{y}_p = \sum_{k=1, k \neq i}^K \left\{ (C^{i,k}(1)+1) \tau^k - 1 \right\} \Re\left\{ \boldsymbol{\delta}_p^* e^{j(\phi_p^k + \theta^k)} \right\} \tag{23}$$

$\alpha = 2\lambda E_s / N$ , and  $\boldsymbol{\delta}_p = \mathbf{g}_p - \tilde{\mathbf{g}}_p$ . Notice that the time delay  $\tau^k$  is normalized by the chip period  $T_c$ .

In the GQR formulation [18], we need to obtain the moments of random variable  $\mathbf{y}_p$  in order to evaluate the expectation of (22); the detail derivations of the moments of random variable  $\mathbf{y}_p$  are given in Appendix C. Based on  $N_m (= 2N_c + 1)$  moments of random variable  $\mathbf{y}$ , the pairs of weight  $W_j$  and node  $\zeta_i$  of size  $N_c$  are obtained in order to specify the expectation of (22) [18]. Hence, from (19), by letting  $\lambda' = \lambda / N_0$  and dropping the primes, we can obtain the pairwise error probability of quasi-synchronous system (13).

## APPENDIX C

### MOMENTS OF $\mathbf{y}_p$ IN (22)

At (22), assuming that the unknown random variable  $\mathbf{y}_p$  and its moments are independent from one symbol period to next period, we can drop the subscript  $p$  from the random variable. Let us define the random variable  $\mathbf{y}$  as

$$\mathbf{y} = \Re\{\boldsymbol{\delta}^* z\} = \frac{\boldsymbol{\delta}^* z + \boldsymbol{\delta} z^*}{2} \tag{24}$$

where

$$z = \sum_{k=1, k \neq i}^K \tilde{R}^{i,k}(\tau^k) e^{j\phi^k} e^{j\theta^k} = \sum_{k=1, k \neq i}^K r_k e^{j\theta^k}$$

$\boldsymbol{\delta} = \mathbf{g} - \tilde{\mathbf{g}}$ , and  $r_k = \tilde{R}^{i,k}(\tau^k) e^{j\phi^k}$ ; and the  $k$ th user signal phase term is  $\phi^k = \{0, 2\pi/M, \dots, 2(M-1)\pi/M\}$  and the phase delay  $\theta^k$  is a random variable that is uniformly distributed for a range of  $0 \sim 2\pi$ . The moments of the random variable  $\mathbf{y}$  are given by

$$E[\mathbf{y}^m] = E\left[\left\{ \frac{\boldsymbol{\delta}^* z + \boldsymbol{\delta} z^*}{2} \right\}^m\right] \tag{25}$$

in which  $m = 1, \dots, N_m$ . The  $N_m$  moments, where  $N_m = 2N_c + 1$ , of  $\mathbf{y}$  yield  $N_c$  pairs of weight  $W_j$  and node  $\zeta_j$  in order to calculate the second expectation on the right hand of (19). Assuming the density function of random variable  $\mathbf{y}$  is even, we need to evaluate just even moments of that r.v.

Let us calculate the even moments of  $\mathbf{y}$  as follows:

$$\begin{aligned} E[\mathbf{y}^{2m}] &= \frac{1}{4^m} E \left[ \sum_{n=0}^{2m} \binom{2m}{n} (\delta^* z)^n (\delta z^*)^{2m-n} \right] \\ &= \frac{1}{4^m} \sum_{n=0}^{2m} \binom{2m}{n} (\delta^*)^n \delta^{2m-n} \cdot E[z^n (z^*)^{2m-n}] \end{aligned} \quad (26)$$

in which the expectation on the right hand of (26) becomes

$$\begin{aligned} & E[z^n (z^*)^{2m-n}] \\ &= E \left[ \left\{ \sum_{\substack{k=1 \\ k \neq i}}^K r_k e^{j\theta^k} \right\}^n \left\{ \sum_{\substack{k=1 \\ k \neq i}}^K r_k^* e^{-j\theta^k} \right\}^{2m-n} \right] \\ &= E \left[ \sum_{\substack{\mathbf{a} \in \mathbf{A} \\ a_k \in \mathbf{a}, k \neq i}} \frac{n!}{a_1! \dots a_K!} (r_1)^{a_1} \dots (r_K)^{a_K} e^{j\theta^1 a_1} \dots e^{j\theta^K a_K} \right. \\ &\quad \left. \cdot \sum_{\substack{\mathbf{b} \in \mathbf{B} \\ b_k \in \mathbf{b}, k \neq i}} \frac{(2m-n)!}{b_1! \dots b_K!} (r_1^*)^{b_1} \dots (r_K^*)^{b_K} e^{-j\theta^1 b_1} \dots e^{-j\theta^K b_K} \right] \end{aligned} \quad (27)$$

where  $i$  is the desired user index;  $a_k$  and  $b_k$  are nonnegative integers and  $\mathbf{A}$  is the set of sequence  $\mathbf{a} = \{a_k | k = 1, \dots, K, \text{ and } k \neq i\}$  such that  $\sum_{k, k \neq i} a_k = n$ , and  $\mathbf{B}$  is the set of sequence  $\mathbf{b} = \{b_k | k = 1, \dots, K, \text{ and } k \neq i\}$  such that  $\sum_{k, k \neq i} b_k = 2m - n$ . Observing (27), there is non-zero only if  $a_k = b_k$ , for  $k = 1, \dots, K$  and  $k \neq i$ . Therefore  $m = n$  and  $\sum_{k, k \neq i} a_k = \sum_{k, k \neq i} b_k = m$ .

Reorganizing (27) gives

$$\begin{aligned} E[z^n (z^*)^{2m-n}] &= \sum_{\substack{\mathbf{a} \in \mathbf{A} \\ a_k \in \mathbf{a}, k \neq i}} \left( \frac{m!}{a_1! \dots a_K!} \right)^2 \\ &\quad \cdot \prod_{k=1, k \neq i}^K E[\{\tilde{R}^{i,k}(\tau^k)\}^{2a_k}]. \end{aligned} \quad (28)$$

As a result, substituting (28) into (26) shows

$$E[\mathbf{y}^{2m}] = \frac{1}{4^m} \binom{2m}{m} \|\boldsymbol{\delta}\|^{2m} \sum_{\substack{\mathbf{a} \in \mathcal{A} \\ a_k \in \mathbf{a}, k \neq i}} \left( \frac{m!}{a_1! \cdots a_K!} \right)^2 \cdot \prod_{k=1, k \neq i}^K E[\{\tilde{R}^{i,k}(\tau^k)\}^{2a_k}]. \quad (29)$$

## REFERENCES

- [1] G. Ungerboeck, "Channel coding with multilevel/phase signals," *IEEE Trans. Inform. Theory*, vol. 28, pp. 55-67, Jan. 1982.
- [2] S. V. Hanly, "Capacity and power control in spread spectrum macrodiversity radio networks," *IEEE Trans. Commun.*, vol. 44, pp. 247-256, Feb. 1996.
- [3] R. Prasad, A. Kegel, and M. G. Jansen, "Effect of imperfect power control on cellular code division multiple access system," *Elect. Lett.*, vol. 28, pp. 848-849, Apr. 23, 1992.
- [4] A. J. Viterbi, *CDMA principles of spread spectrum communication*, Addison-Wesley Publishing Company, 1st Edition, 1995.
- [5] I. Ghauri and R. A. Iltis, "Capacity of the linear decorrelating detector for QS-CDMA," *IEEE Trans. Commun.*, vol. 45, pp. 1039-1042, Sep. 1997.
- [6] J. L. Massey and T. Mittelholzer, "Welch's bound and sequence sets for code-division multiple access systems," in *Sequences II, Methods in Communication, Security and Computer Science*, R. Capocelli, A. De Santis, and U. Vaccaro, Eds. New York: Springer-Verlag, 1993.
- [7] R. D. Gaudenzi and F. Giannetti, "Analysis and performance evaluation of synchronous trellis-coded CDMA for satellite applications," *IEEE Trans. Commun.*, vol. 43, pp. 1400-1408, Feb./Mar./Apr. 1995.
- [8] R. D. Gaudenzi, C. Elia, and R. Viola, "Bandlimited quasi-synchronous CDMA: a novel satellite access technique for mobile and personal communication systems," *IEEE J. Select. Areas Commun.*, vol. 8, pp. 328-343, Feb. 1992.
- [9] G. D. Boudreau, D. D. Falconer, and S. A. Mahmoud, "A comparison of trellis coded versus convolutionally coded spread-spectrum multiple-access systems," *IEEE J. Select. Areas Commun.*, vol. 8, pp. 628-639, May 1990.
- [10] G. D. Boudreau, "Analysis of the application of trellis coding to spread spectrum multiple access systems," Ph.D. dissertation, Dept. Sys. Comput. Eng., Carleton Univ., Ottawa, Canada, 1989.
- [11] P. K. Enge and D. V. Sarwate, "Spread spectrum multiple-access performance of orthogonal codes - linear receivers," *IEEE Trans. Commun.*, vol. 35, pp. 1309-1318, Dec. 1987.
- [12] H. Yamamura and R. Kohno, "Analysis of CDMA with multidimensional coded modulation in fading channel," *Proc. IEEE ICUPC '95*, Tokyo, Japan, pp 246-250, Nov. 1995.
- [13] S. S. Pietrobon, R. H. Deng, A. Lafranechere, G. Ungerboeck, and D. J. Costello, "Trellis-coded multidimensional phase modulation," *IEEE Trans. Inform. Theory*, vol. 36, pp. 63-89, Jan. 1990.
- [14] G. D. Forney, "Geometrically uniform codes," *IEEE Trans. Inform. Theory*, vol. 37, pp. 1241-1260, Sep. 1991.
- [15] B. D. Woerner and W. E. Stark, "Trellis-coded direct-sequence spread-spectrum communications," *IEEE Trans. Commun.*, vol. 42, pp. 3161-3170, Dec. 1994.
- [16] M. B. Pursley, "Spread spectrum multiple access communications," in *Multi-User Communications*, G. Longo, Ed. Vienna and New York: Springer-Verlag, pp. 139-199, 1981.
- [17] M. G. Jansen and R. Prasad, "Capacity, throughput, and delay analysis of a cellular DS CDMA system with imperfect power control and imperfect sectorization," *IEEE Trans. Veh. Technol.*, vol. 42, pp. 67-75, Feb. 1995.
- [18] M. Kavehrad, "Performance of nondiversity receivers for spread spectrum in indoor wireless communications," *AT&T Tech. J.*, vol. 64, pp. 1181-1210, July-Aug. 1985.
- [19] E. Biglieri, "High-level modulation and coding for nonlinear satellite channels," *IEEE Trans. Commun.*, vol. 32, pp. 616-626, May 1984.
- [20] D. Divsalar and M. K. Simon, "Trellis coded modulation for 4800-9600 bits/s transmission over a fading mobile satellite channel," *IEEE J. Select. Areas Commun.*, vol. 5, pp. 162-174, Feb. 1987.
- [21] D. N. Knisely, S. Kumar, S. Laha, and S. Nanda, "Evolution of wireless data services: IS-95 to cdma2000," *IEEE Commun. Mag.*, vol. 36, pp. 140-149, Oct. 1998.

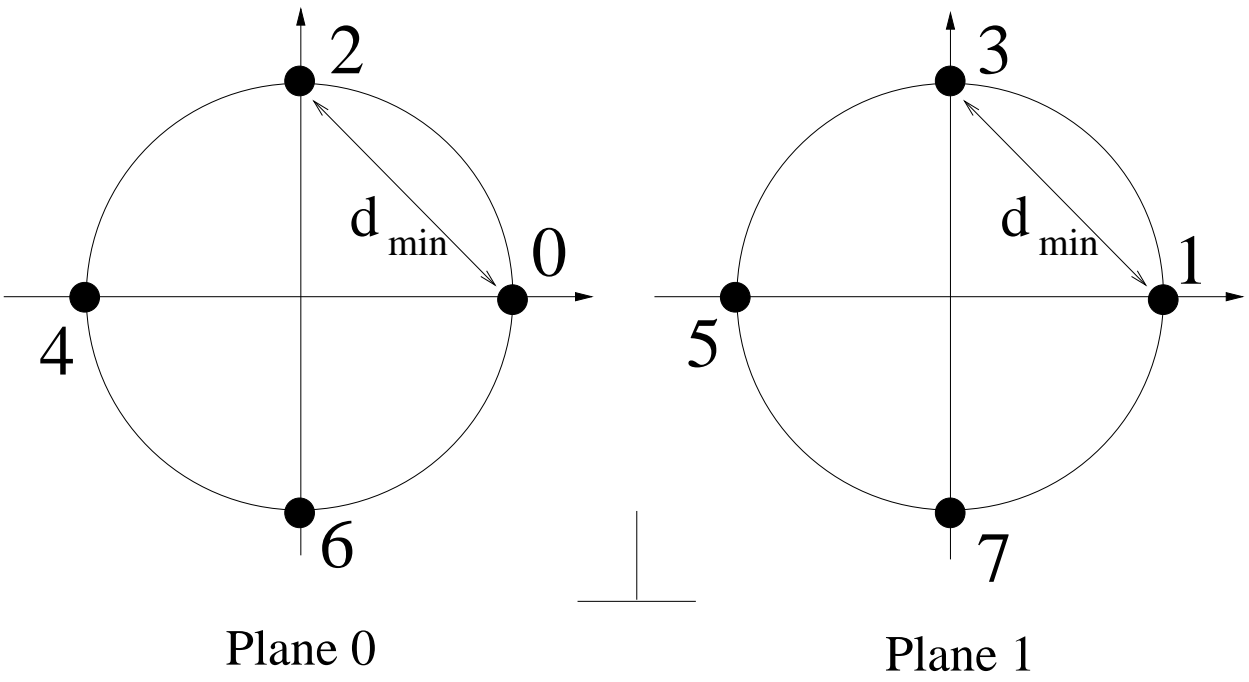


Fig. 1. Signal constellation for 2P4PSK.

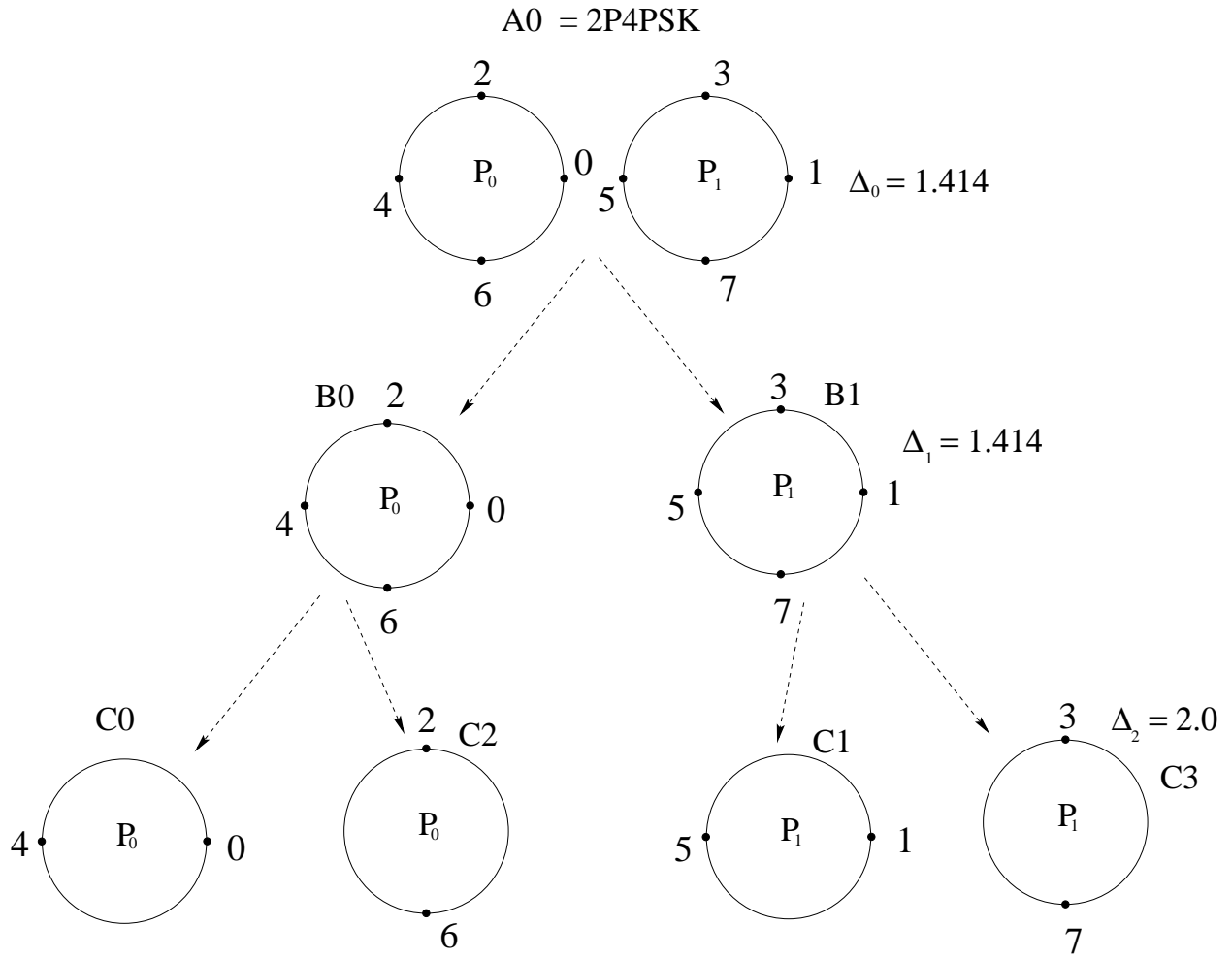


Fig. 2. Set partitioning of 2P4PSK.

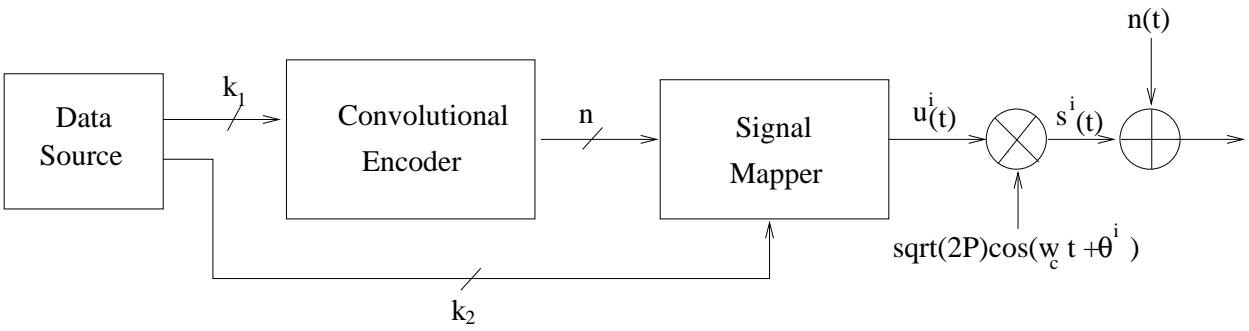


Fig. 3. Transmitter block diagram of trellis coded system.

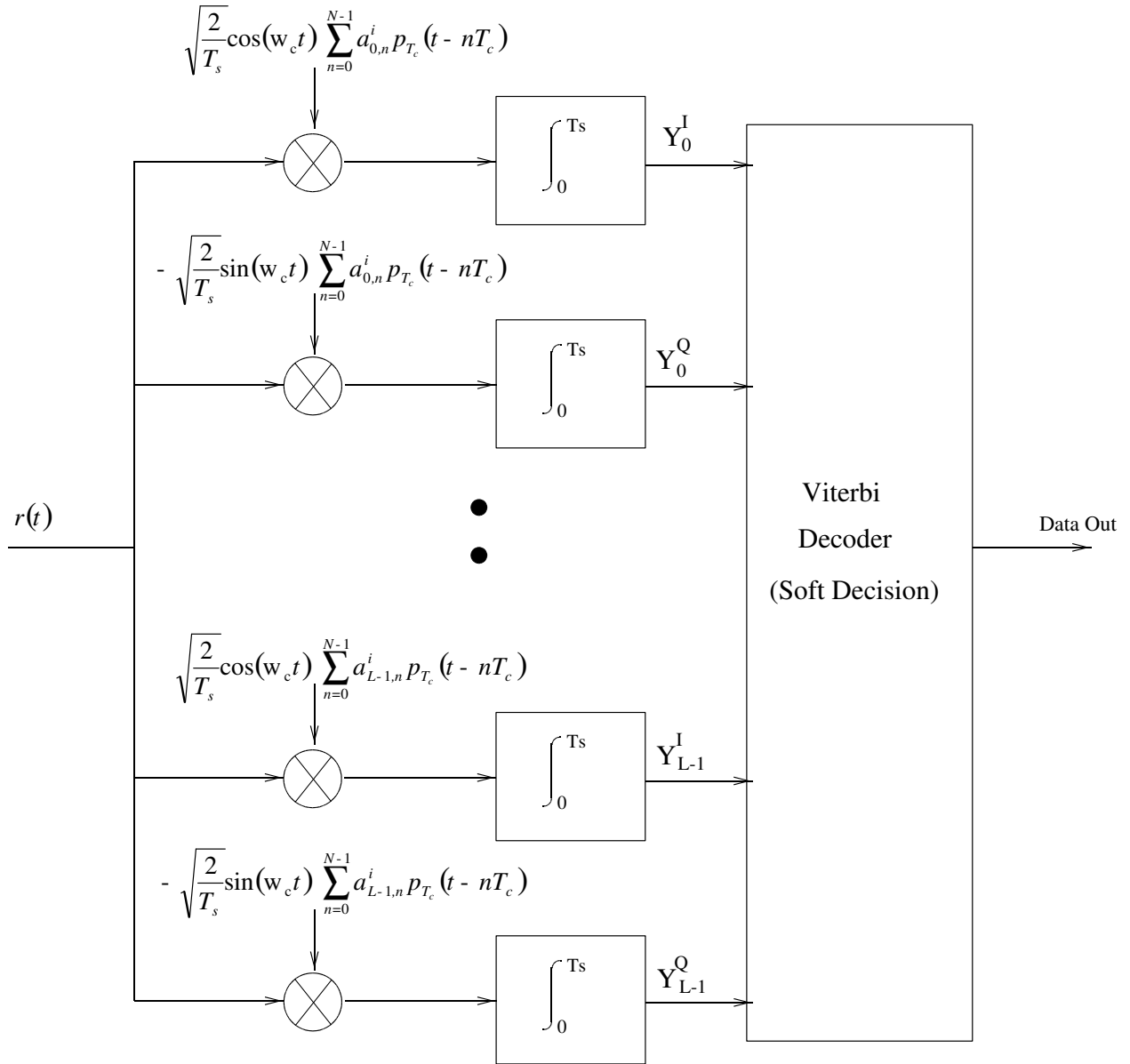


Fig. 4. Receiver block diagram of trellis coded system.

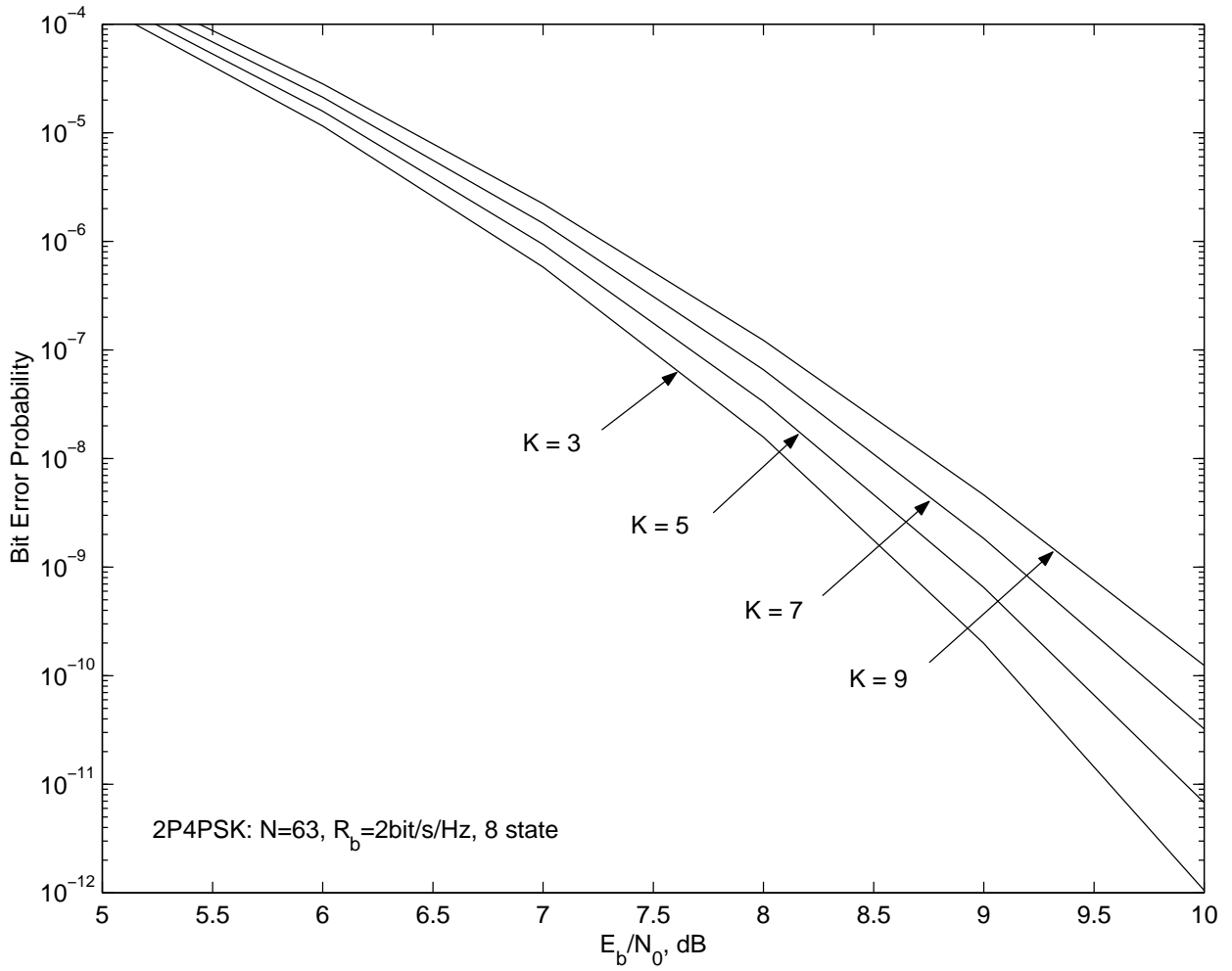


Fig. 5. Upper bounds on bit error probability of quasi-synchronous 2/3 2P4PSK TC with 8-state 2/3 convolutional code as a function of number of users ( $K$ ).

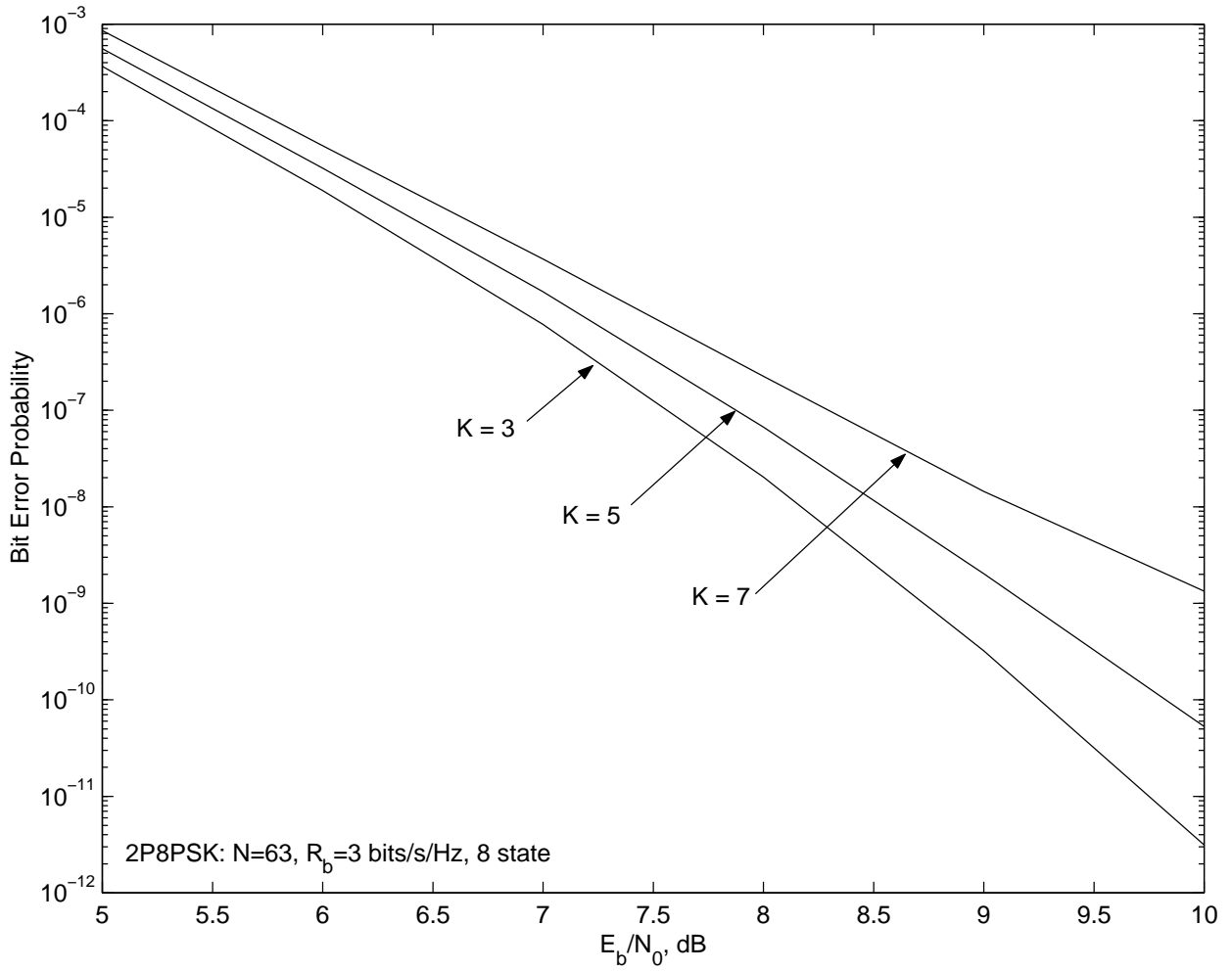


Fig. 6. Upper bounds on bit error probability of quasi-synchronous 3/4 2P8PSK TC with 8-state 2/3 convolutional code as a function of number of users ( $K$ ).

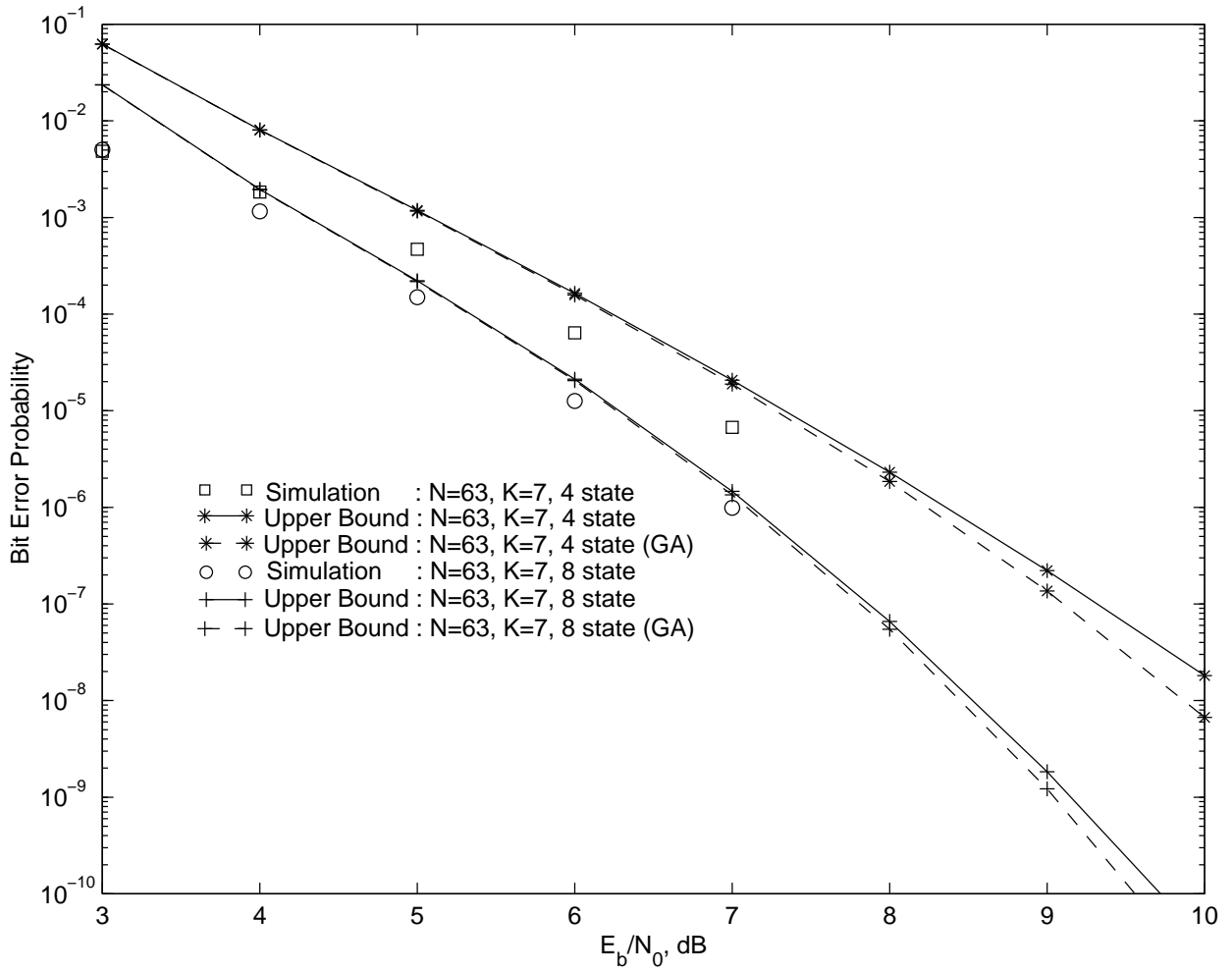


Fig. 7. Comparison between simulation results and theoretical upper bounds of quasi-synchronous 2/3 2P4PSK TC.

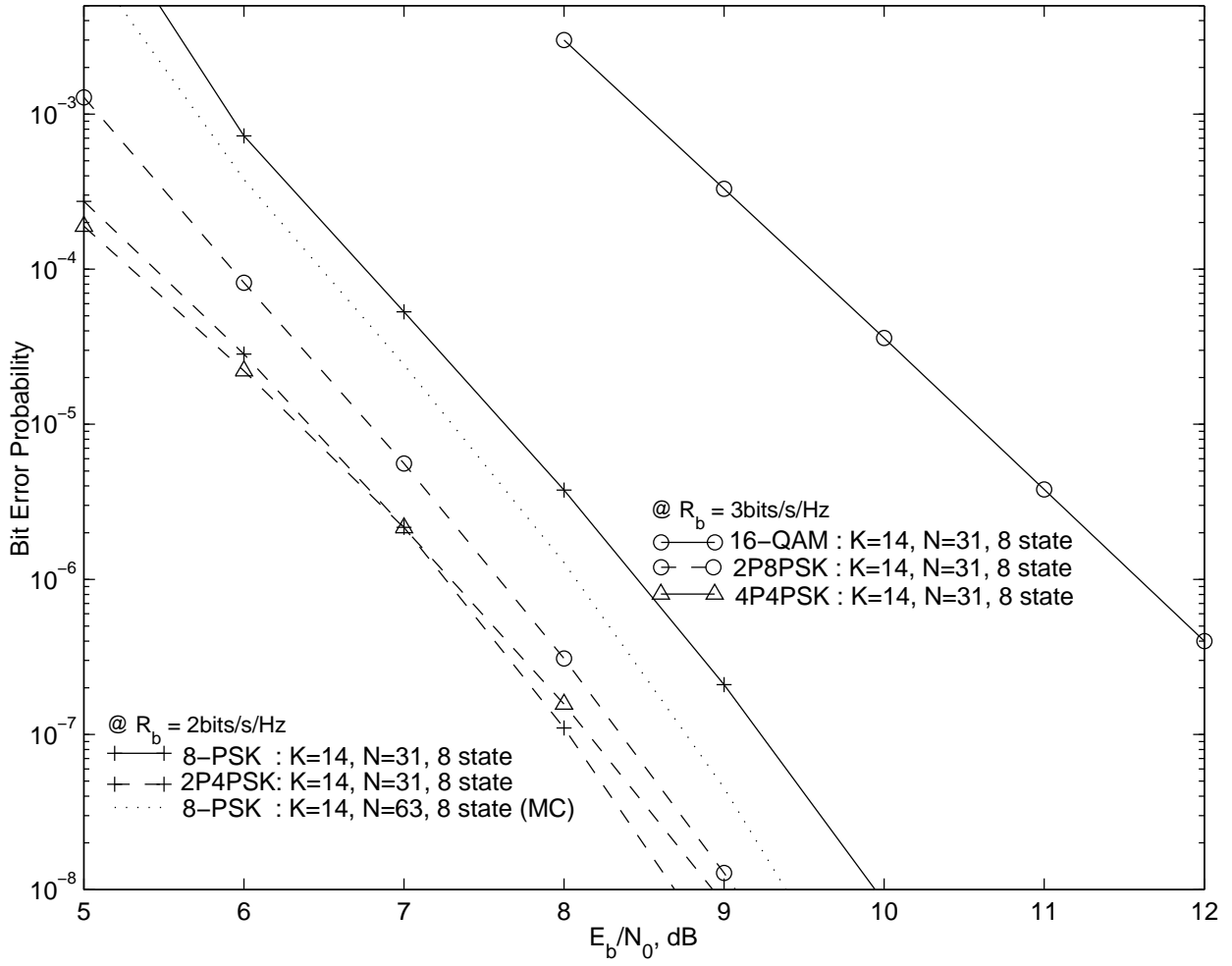


Fig. 8. Comparison between conventional TC, conventional multi-code TC schemes, and OPSM TC schemes both at rate 2/3 TC and at rate 3/4 TC, respectively, with the same 8-state 2/3 convolutional code.

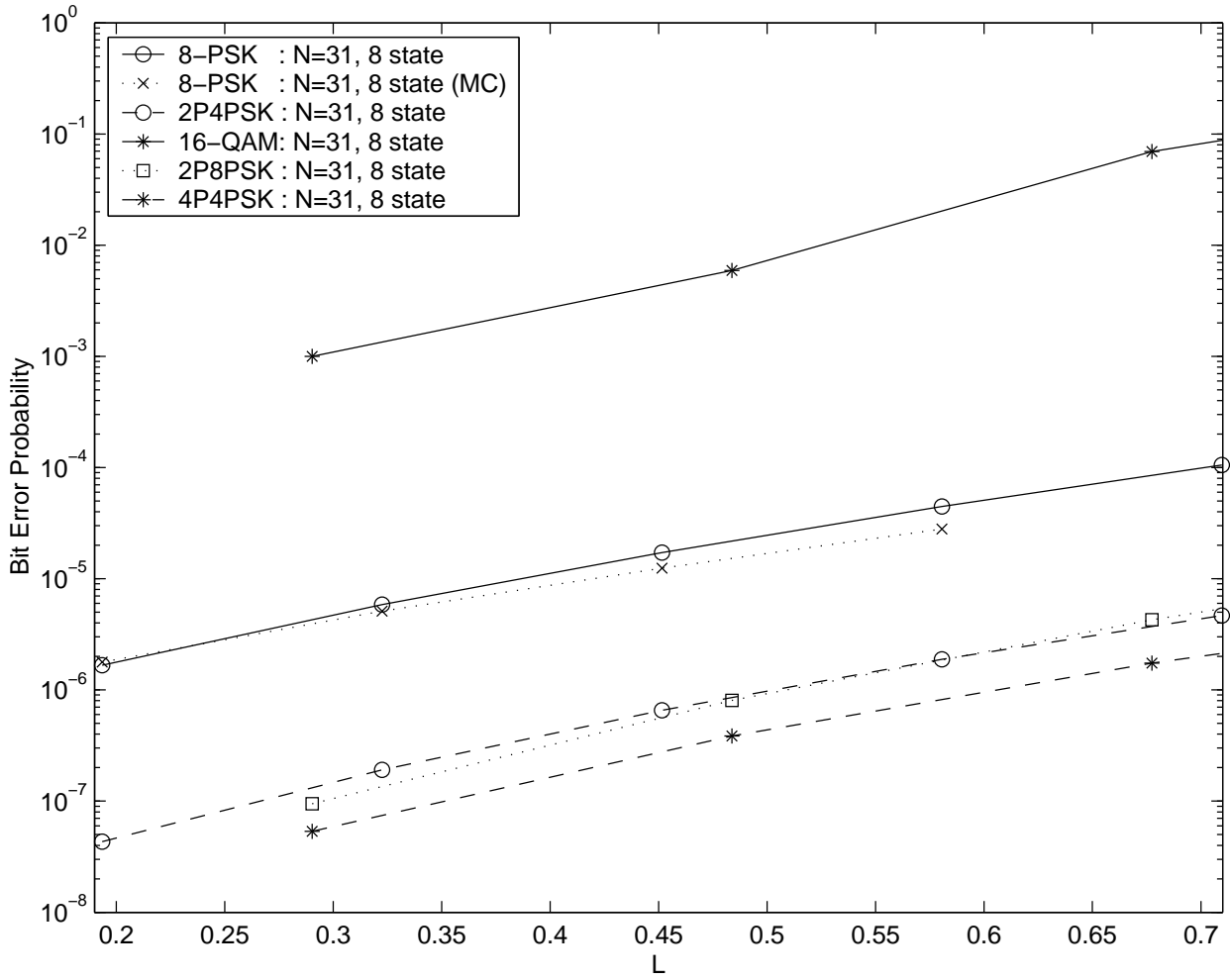


Fig. 9. BER performance as a function of normalized offered traffic  $L (= R_b * K/N)$  for conventional TC, conventional multi-code TC schemes, and OPSM TC schemes both at rate  $2/3$  TC and at rate  $3/4$  TC, respectively, with the same 8-state  $2/3$  convolutional code.